Neuroprotective Effects of Metallothionein Against Rotenone-induced Myenteric Neurodegeneration in Parkinsonian Mice

Shinki Murakami[a], Ikuko Miyazaki[a], Norio Sogawa[b], Ko Miyoshi[a, #], Masato Asanuma[a, *]

[a] Department of Brain Science, [b] Department of Dental Pharmacology, Okayama University Graduate School of Medicine, Dentistry and Pharmaceutical Sciences, Okayama, Japan

* **Corresponding author**:

Masato Asanuma, MD, PhD,

Department of Brain Science, Okayama University Graduate School of Medicine, Dentistry and Pharmaceutical Sciences, 2-5-1, Shikata-cho, Kita-ku, Okayama, 700-8558, Japan.

Phone: (+81) 86-235-7408, Fax: (+81) 86-235-7412,

E-mail address: asachan@cc.okayama-u.ac.jp

[#] Current address: Molecular Research Center for Children's Mental Development, Department of Child Development and Molecular Brain Science, United Graduate School of Child Development, Osaka University, Suita, Osaka, Japan

Abbreviations

ANOVA, analysis of variance; ChAT, choline acetyltransferase; CNS, central nervous system; DAT, dopamine transporter; DMSO, dimethylsulphoxide; ENS, enteric nervous system; GFAP, glial fibrillary acidic protein; KO, knockout; LB, Lewy-body; LN, Lewy-neurite; MT, metallothionein; PB, phosphate buffer; PBS-T, phosphate buffered saline with 0.2% Triton X-100; PD, Parkinson's disease; PEG, polyethylenglycol; RT, room temperature; SNpc, substantia nigra pars compacta; TH, tyrosine hydroxylase; WT, wild type; 4HNE, 4-hydroxynonenal

Abstract

Parkinson's disease (PD) is a neurodegenerative disease with motor symptoms as well as non-motor symptoms that precede the onset of motor symptoms. Mitochondrial complex I inhibitor, rotenone, has been widely used to reproduce PD pathology in the central nervous system (CNS) and enteric nervous system (ENS). We reported previously that metallothioneins (MTs) released from astrocytes can protect dopaminergic neurons against oxidative stress. The present study examined the changes in MT expression by chronic systemic rotenone administration in the striatum and colonic myenteric plexus of C57BL mice. In addition, we investigated the effects of MT depletion on rotenone-induced neurodegeneration in CNS and ENS using MT-1 and MT-2 knockout (MT KO) mice, or using primary cultured neurons from MT KO mice. In normal C57BL mice, subcutaneous administration of rotenone for 6 weeks caused neurodegeneration, increased MT expression with astrocytes activation in the striatum and myenteric plexus. MT KO mice showed more severe myenteric neuronal damage by rotenone administration after 4 weeks than wild-type (WT) mice, accompanied by reduced astroglial activation. In primary cultured mesencephalic neurons from MT KO mice, rotenone exposure induced neurotoxicity in dopaminergic neurons, which was complemented by addition of recombinant protein. The present results suggest that MT seems to provide protection against neurodegeneration in ENS of rotenone-induced PD model mice.

Key Words: Parkinson's disease; rotenone; enteric nervous system; astrocytes; metallothionein

Introduction

Parkinson's disease (PD) is a progressive neurodegenerative disease with motor symptoms, such as tremor, bradykinesia, rigidity, and postural instability that are based on selective loss of nigrostriatal dopaminenergic neurons, and with non-motor symptoms such as dysosmia, orthostatic hypotension and constipation. Lewy-bodies (LBs) and Lewy-neurites (LNs) are pathological hallmarks of PD, which are cytoplasmic inclusions of insoluble, aggregated proteins, including major component α-synuclein (Spillantini et al. 1997). Braak *et al.* and other groups reported that LBs and LNs exist in not only the nigrostriatal pathway, but also the olfactory bulb in the central nervous system (CNS), dorsal motor nucleus of the vagus, cardiac sympathetic nerves and myenteric neurons in the enteric nervous system (ENS) (Braak et al. 2003; Hubbard et al. 2007; Orimo et al. 2008).

Although the pathogenic mechanisms of PD remain to be elucidated, evidence suggests the involvement of mitochondrial dysfunction and oxidative stress in the substantia nigra (Parker et al. 1989; Schapira et al. 1989; Sofic et al. 1992). Rural life, agricultural work life and exposure to pesticides are possible environmental risk factors for PD (Wong et al. 1991; Tanner et al. 2011). Rotenone is a natural pesticide, a mitochondrial complex I inhibitor, and previous reports indicated that users of rotenone or agricultural workers were at higher risk of PD and associated gastrointestinal neuropathology (Dhillon et al. 2008). Previous experimental studies have demonstrated that long-term systemic administration of rotenone in rats produced many features of PD pathology. For example, Betarbet *et al*. reported that long-term systemic administration of rotenone in Lewis rats replicated the hallmarks of PD, including selective nigrostriatal dopaminergic neurodegeneration, formation of LBs in the substantia nigra and parkinsonian motor dysfunction (Betarbet et al. 2000). In addition, long-term treatment with rotenone caused gastrointestinal dysfunction in rats (Greene et al. 2009). Direct intragastric administration of rotenone in mice resulted in accumulation and

aggregation of α-synuclein in neurons of the dorsal motor nucleus of the vagus and intermediolateral nucleus of the spinal cord, accompanied by neuronal loss and astrogliosis (Pan-Montojo et al. 2010). Thus, rotenone has been widely used to reproduce PD pathology in CNS and ENS.

Metallothioneins (MTs) are a family of low-molecular weight, cysteine-rich and inducible intracellular proteins, and are known to be involved in homeostasis and detoxification of heavy metals and scavenging of free radicals. MTs have neuroprotective effects in various neurological disorders of both the CNS and ENS (Stankovic et al. 2007; Pedersen et al. 2009). We have previously demonstrated that MT-1 and MT-2 have neuroprotective roles against dopaminergic neuronal damage in an animal model of PD (Asanuma et al. 2002) and that MTs released from astrocytes is a potent protector of dopaminergic neurons against oxidative stress (Miyazaki et al. 2011; 2013). Up-regulation of MT expression in reactive astrocytes has been reported in the substantia nigra of PD patients, suggesting the involvement of astrocytes in mediating the neuroprotective effects of MTs (Michael et al. 2011).

The present study was designed to elucidate the MT expression after long-term subcutaneous administration of rotenone in CNS and ENS of C57BL mice. We also investigated the role of MT in the rotenone-induced pathological changes in ENS using MT knockout (KO) mice, and the neuroprotective effect of MT using primary cultured neurons.

Materials and Methods

Animals

Male C57BL/6J mice weighting 20-25 g (9-week-old) were purchased from Japan Charles River Laboratories Japan, Inc. (Yokohama, Japan). Male homozygous MT-1 and MT-2 knockout (MT KO) mice with simultaneous disruption of both MT-1 and MT-2 genes

(Masters et al., 1994) were purchased from the Jackson Laboratories (#2211: 129S7/SvEvBrd-MT1^{tm1Bri}MT2^{tm1Bri}/J; Bar Harbor, ME). The 129/Sv mice were employed as WT controls, since the MT KO mice were raised on a 129/Sv genetic background. The animals were acclimated to and maintained at 23°C under a 12-h light/dark cycle (lights on 08:00-20:00 h). Mice were housed in standard laboratory cages and had free access to food and water throughout the study period. All animal procedures were in strict accordance with the NIH Guide for the Care and Use of Experimental Animals and the Guideline for Animal Experiments of Okayama University Advanced Science Research Center, and were approved by the Animal Care and Use Committee of Okayama University Advanced Science Research Center. Special interest was taken to minimize the number of animals used in this research.

Administration of Rotenone

Rotenone (Sigma, St. Louis, MO) was dissolved in vehicle solution [dimethylsulphoxide (DMSO) and polyethylenglycol (PEG) (1:1)], and then poured into the tank of an osmotic mini pump (Alzet, #2004; Durect Corporation, Cupertino, CA). Mice (9-week-old) were anesthetized with sodium pentobarbital (60 mg/kg, i.p.) and the osmotic pump was implanted under the skin of the back. The dose of infused rotenone was 50 mg/kg/day calculated by average body weight and at a delivery rate of 0.25 μl/h. For the control group, the same volume of vehicle (DMSO:PEG = 1:1) was infused using the subcutaneously implanted osmotic pump.

Body Weight and Behavioral Test

Spontaneous locomotor activity was observed in a circular open field measuring 60-cm in diameter with a surrounding 50-cm high wall. The bottom was divided into two equal concentric zones with 18 areas of equal extension. Each animal was placed in the middle of

the openfield at daytime every week after pump implantation, and then the number of line crossing per 3 min were counted. All observations were performed during the daytime within the same time (15:00-17:00 h).

Tissue Collection and Preparation

After the experimental period, mice were deeply anesthetized with sodium pentobarbital (80 mg/kg, i.p.) and perfused intracardially with ice-cold saline. The brain and the colon were rapidly removed and post-fixed in a Histochoice Tissue Fixative (Sigma) overnight at 4°C. The brains were cryoprotected in 15% sucrose in 0.1 M sodium phosphate buffer (PB; pH 7.4) with 0.1% sodium azide, and then coronal frozen sections (20-μm-thick) were prepared at levels containing the substantia nigra pars compacta (SNpc: -2.8 to -3.0 mm from the bregma) or the mid-striatum (+0.6 to +1.0 mm from the bregma) using a cryostat. The ascending colon samples were rinsed briefly in saline, dehydrated, and embedded in paraffin. The paraffin-embedded tissue sections were cut (4-μm-thick) by a microtome.

Immunohistochemistry of Mouse Tissue Sections

The brain sections were soaked in 0.5% hydrogen peroxide in 10 mM phosphate buffered saline with 0.2% Triton X-100 (PBS-T), followed by incubation in 1% normal goat serum for 30 min at room temperature (RT). Then, they were reacted with rabbit anti-tyrosine hydroxylase (TH; dilution 1:1000; Chemicon International, Temecula, CA) or rat anti-dopamine transporter (DAT; 1:1000; Chemicon International) overnight at 4°C. After extensive rinsing in PBS-T, the sections were reacted with goat biotinylated anti-rabbit IgG secondary antibody (1:500; Vector Laboratories, Burlingame, CA) or rabbit biotinylated anti-rat IgG secondary antibody (1:1000; Vector Laboratories) for 2 h at RT, and then incubated with avidin-biotin peroxidase complex (1:1000, Vector Laboratories) for 1 h at RT.

For visualizing of TH-immunopositive cells, the sections were soaked in a solution containing 3,3'-diaminobenzidine, nickel, and hydrogen peroxide.

For immunofluorescence staining, the brain sections were placed in 1% normal goat serum for 30 min at RT, and then incubated with rabbit anti-glial fibrillary acidic protein (GFAP) polyclonal antibody (1:1000; Dako Cytomation, Glostrup, Denmark) and mouse anti-MT (1:100; Dako Cytomation) overnight at 4°C. The sections were incubated for 2 h at RT with goat anti-rabbit IgG conjugated to Alexa Fluor 488 (1:1000; Molecular Probes, Eugene, OR) and goat anti-mouse IgG conjugated to Alexa Fluor 594 (1:1000; Molecular Probes).

For immunostaining of colonic sections, the sections were deparaffinized, and then activated by autoclave for 5 min at 120°C. After return to RT, the sections were placed in 10% normal goat serum or donkey serum for 10 min, and then incubated overnight with primary antibody of rabbit anti-TH (1:200; Millipore, Temecula, CA), mouse anti-HuC/D (10 μg/ml; Molecular Probes), rabbit anti-β-tubulin (1:200; GeneTex, Tokyo, Japan), goat anti-choline acetyltransferase (ChAT; 1:200; Chemicon International), rabbit anti-GFAP (1:200; Dako Cytomation), mouse anti-GFAP (1:200; Millipore), goat anti-GFAP (1:200; Abcam), rabbit anti-MT (1:200; Santa Cruz Biotechnology, Santa Cruz, CA), or goat anti-4-hydroxynonenal (4HNE; 1:200; Abcam, Cambridge, UK) polyclonal antibody at 4°C. The sections were incubated with goat anti-mouse IgG conjugated to Alexa Fluor 594 or Alexa Fluor 488, goat anti-rabbit IgG conjugated to Alexa Fluor 488 or donkey anti-goat IgG conjugated to Alexa Fluor 594 (1:200; Molecular Probes) for 30 min at RT.

Primary Culture of Neurons

Primary cultured neurons were prepared from the mesencephalon of MT KO mice embryos at 15 days. The cells from the mesencephalon were plated in Dulbecco's modified Eagle's

medium (Invitrogen, San Diego, CA) containing 10% fetal bovine serum at a density of 2 × 10^5 cells/cm^2 in 4-chamber culture slides coated with poly-D-lysine (Becton Dickinson Labware, Franklin Lakes, NJ). Within 24 h after initial plating, the medium was replaced with fresh medium supplemented with 2 μM cytosine-β-D-arabinofuranoside to inhibit the replication of non-neuronal cells, followed by incubation for a further 7 days. In neuron-rich cultures, 95% of the cells were immunoreactive for the neuronal marker microtubule-associated protein 2.

Cell Treatments

To identify whether MT can protect dopaminergic neurons against rotenone-induced neurotoxicity, the primary cultured mesencephalic neurons from MT KO mice were treated with rotenone (final concentration 5 nM) and rabbit MT-1 recombinant protein (final concentration 25 ng/ml; ENZO Life Sciences, Farmingdale, NY) for 24 h.

Immunocytochemistry of Primary Cultured Neurons

The cells on the chamber slides were fixed with 4% paraformaldehyde for 20 min, blocked with 2.5% normal goat serum for 20 min, and reacted with mouse anti-TH (1:1000; Millipore) for 18 h at 4°C. The secondary antibodies used were goat anti-mouse IgG conjugated to Alexa Fluor 594. The cells were counterstained with Hoechst nuclear stain (10 μg/ml) for 2 min and washed before mounting with Fluoromounting medium (Dako Cytomation).

Image Analysis

The number of TH-immunopositive neurons in the SNpc of a midbrain section (-2.8 to -3.0 mm from the bregma) was counted and TH or DAT-immunoreactivity in the mid-striatum

(+0.6 to +1.0 mm from the bregma) were measured using a microscope and an image analysis system (NIH Image J 1.44K, Bethesda, MD) at x200 or x40 magnification, respectively. The boundary between the substantia nigra pars compacta and ventral tegmental area was defined by a line extending dorsally from the most medial boundary of the cerebral peduncle. Striatal GFAP and MT-immunopositive astrocytes were counted using a fluorescence microscope at x200 magnification. In the brain sections, the number of immunopositive cells or the optical density of immunoreactivity from the left and right image was averaged for all sections analysed. The TH, GFAP, MT, HuC/D, β-tubulin, ChAT and 4HNE-immunoreactivity in the myenteric plexus of the colon (10-30 images/2 sections at different level/animal, 4-7 animals/group) were observed using a fluorescence microscope at x400 magnification and quantified by NIH Image J 1.44K. The integrated density of each signal was calculated as follows: integrated density = (signal density in the myenteric plexus - background density in the adjacent muscle layer) x area of positive signal in the plexus. The number of HuC/D-immunopositive cells in the myenteric plexus of a colonic sections was counted using a fluorescence microscope at x400 magnification. All slides for immunofluorescence staining were analyzed under a fluorescence microscope. They were used a mercury lamp through a 470-490 nm and 530-550 nm band-pass filters to excite Alexa Fluor 488 and Alexa Fluor 594, respectively. The light emitted from Alexa Fluor 488 and Alexa Fluor 594 was collected through 515-550 nm band-pass filters or 590 nm long-pass filters, respectively. TH-immunopositive cells on chamber slides were counted and were calculated in 10 to 12 randomly chosen fields under the microscope. Counting was performed blindly.

Statistical Analysis

Values were expressed as mean±SEM. Differences among groups were examined by one-way analysis of variance (ANOVA) followed by *post-hoc* Tukey-test (J STAT software). A *p* value

less than 0.05 was considered statistically significant.

Results

Effects of Subcutaneous Rotenone administration on Spontaneous Locomotor Activity in C57BL Mice

Subcutaneous administration of rotenone for up to 6 weeks had no effect on body weight of C57BL mice (Fig. 1a). While, it showed a significant decrease in spontaneous locomotor activity compared with vehicle-treated C57BL mice at 2, 5 and 6 weeks (Fig. 1b).

Effects of Rotenone on Dopaminergic Neurons, Astrocytes and MT Expression in the Striatum

We used TH-immunohistochemistry as a marker of dopaminergic neurons. Treatment with rotenone for 6 weeks decreased the optical density of striatal TH-immunoreactivity (Fig. 2a). In addition, the number of GFAP-positive astrocytes were increased (Fig. 2b) and MT-positive cells (Fig. 2c) tended to increase, and these signals were partly colocalized (Fig. 2d) in the striatum at 6 week of subcutaneous rotenone administration.

Effects of Rotenone on Myenteric Neurons, Glial Cells and MT Expression

Administration of rotenone for 6 weeks resulted in decrease in TH-immunoreactive integrated density in the ascending colon of C57BL mice (Fig. 3a). Rotenone tended to increase GFAP-immunopositive integrated density in the myenteric plexus of the colon at 6 weeks (Fig. 3b). Treatment with rotenone for 6 weeks markedly increased MT-immunopositive integrated density in the myenteric plexus (Fig. 3c).

Effects of Rotenone on Spontaneous Locomotor Activity in MT KO Mice

Administration of rotenone for up to 4 weeks had no effect on body weight of WT 129/Sv

mice and MT KO mice with 129/Sv genetic background (Fig. 4a). Baseline of locomotor activity in vehicle-treated MT KO mice was higher than that in vehicle-treated WT controls (Fig. 4b), implying possible neurodevelopmental changes by MT deficiency. Unlike body weight, the rotenone-induced reduction of spontaneous locomotor activity was much greater in MT KO mice than that in WT 129/Sv mice (Fig. 4b).

Effects of MT Depletion on Rotenone-induced Changes in Dopaminergic Neurons and Astrocytes in the Basal Ganglia

Four-week administration of rotenone caused greater loss of striatal TH- and DAT-immunoreactivities of dopaminergic nerve fibers but not nigral TH-positive neurons in MT KO mice, compared with WT 129/Sv mice (Fig. 5a-c). Furthermore, 4-week administration of rotenone significantly increased the number of GFAP-positive astrocytes in the striatum of WT mice, but not in MT KO mice (Fig. 6a). Reflecting astrocyte activation, 4-week administration of rotenone in WT mice increased the number of striatal MT-positive cells (Fig. 6b). Increased MT-positive signals were partly colocalized with GFAP-positive reactive astrocytes in the striatum of WT mice after rotenone administration (Fig. 6c).

Effects of MT Depletion on Rotenone-induced Changes in Neurons and Glial Cells in ENS

Administration of rotenone for 4 weeks significantly decreased the number of HuC/D-immunopositive neurons and reduced the integrated density of TH-immunopositive signals in colonic myenteric plexuses of WT mice (Fig. 7a and 7c). In addition, in MT KO mice, the rotenone exposure significantly reduced the integrated density of β-tubulin and ChAT-immunopositive signals in colonic myenteric plexuses (Fig. 7b and 7d) as well as the reductions of HuC/D-positive neurons and TH-positive signals. On the other hand, systemic rotenone administration also increased the integrated density of GFAP-immunoreactivity (Fig.

8a) and markedly up-regulated MT-immunoreactivity in the myenteric plexuses of WT mice (Fig. 8b). In contrast to the up-regulation of GFAP signals in WT mice, rotenone markedly reduced myenteric GFAP-immunoreactivity in MT KO mice (Fig. 8a). MT-immunopositive signals were colocalized with GFAP-immunopositive signals (Fig. 8c). We examined myenteric 4HNE-immunoreactivity as a marker of lipid peroxidation by rotenone-induced oxidative stress (Fig. 9a). Subcutaneous rotenone administration significantly increased the ratio of 4HNE to β-tubulin-immunopositive signal in the myenteric plexus in MT KO, compared with WT mice (Fig. 9b).

Neuroprotective Effects of MT against Rotenone-induced Neurotoxicity in Primary Cultured Neurons

In mesencephalic primary cultured neurons from MT KO mice, rotenone (5 nM) exposure significantly decreased the number of TH-positive dopaminergic neurons (Fig. 10). Treatment with MT-1 recombinant protein (5 ng/ml) could attenuate the rotenone-induced toxicity in neurons from MT KO mice.

Discussion

We examined the effects of long-term subcutaneous administration of rotenone on neurons, astroglial cells and MT expression in CNS and ENS in mice. The present study demonstrated that (1) long-term administration of rotenone markedly increased MT expression in the myenteric glial cells, (2) rotenone-induced neuronal loss in the myenteric plexus was more obvious in MT KO mice compared with WT mice, (3) rotenone exposure caused degeneration of primary cultured dopaminergic neurons from MT KO mice, which was attenuated by complement with MT protein.

Several experimental models of PD induced by rotenone have been described

(Betarbet et al. 2000; Sherer et al. 2003; Fleming et al. 2004; Saravanan et al. 2005; Drolet et al. 2009; Greene et al. 2009). The findings in these models suggest that rotenone administration can reproduce several features of PD in both CNS and ENS. Previous studies reported that intragastric administration of rotenone caused accumulation of α-synuclein and PD-like pathology in ENS (Pan-Montojo et al. 2012). To rule out direct damage of the ENS by the toxin, rotenone was infused subcutaneously using an osmotic pump in the present study. At first, we examined MT expression by subcutaneous rotenone administration in CNS and ENS using C57BL mice. In CNS, administration of rotenone for 6 weeks caused significant degeneration of striatal dopaminergic nerve terminal and slight induction of MT. In ENS, rotenone induced significant neurodegeneration and remarkable up-regulation of MT expression in myenteric plexus. Neuronal and glial cells in ENS are generally exposed various environmental factors, such as dietary nutritional and bacterial inflammatory stimuli. Therefore, it is assumed that there is temporal difference of region-specific susceptibility to rotenone toxicity between CNS and ENS.

Astrocytes are abundant in CNS and play various roles to support neurons, such as removal of neurotoxic molecules, synthesis of nutritional factors, constitution of blood brain barrier and production of antioxidants (Heneka et al. 2010). GFAP-positive activated astrocytes are seen in neurodegenerative disorders, suggesting the involvement of astrocytes in various neurodegenerative diseases including PD (Ishida et al. 2006; Durrenberger et al. 2009). In fact, astrogliosis has been described in the brain of PD patients and rotenone-treated rats (Schwarz et al. 1996; Samantaray et al. 2007). Moreover, enteric astroglial cells which express GFAP also exist in ENS (Jessen and Mirsky 1983). It is also reported that enteric glial cells regulate tight-junction integrity and epithelial permeability at mucosal surfaces comparable with blood-brain barrier function (Savidge et al. 2007). Enteric glial cells also have been implicated in the regulation of barrier functions in health and disease conditions.

The present study demonstrated that administration of rotenone in C57BL mice tended to increase GFAP-positive glial cells in the colonic myenteric plexus, as well as in the striatum. This suggests the possible involvement of GFAP-positive activated glial cells in some reactions to the systemic rotenone-induced neurodegeneration in both CNS and ENS.

MT-1 and MT-2 are cysteine-rich metal-binding proteins, which can exert high anti-oxidative activity by scavenging free radicals. MTs are up-regulated specifically in astrocytes in response to neuronal injury (Chung et al. 2004), and are localized in GFAP-positive astrocytes in ischemic lesions (Wakida et al. 2007). We have previously reported that MT-1 and MT-2 provide neuroprotection against 6-hydroxydopamine-induced nigrostriatal neurodegeneration (Asanuma et al. 2002) and against L-DOPA-induced dopamine quinone neurotoxicity in parkinsonian mice (Miyazaki et al. 2007), and recently found that MTs were induced and released in astrocytes, which protect dopaminergic neurons against oxidative stress (Miyazaki et al. 2011; 2013). In addition, MT transgenic mice were reported to be resistant to rotenone-induced neurotoxicity (Ebadi et al. 2005). Other studies demonstrated that mitochondrial oxidative stress specifically induced MTs than other antioxidants, and that MTs scavenged free radicals in mitochondria (Kondoh et al. 2001; Futakawa et al. 2006).

In our study, 4-week administration of rotenone resulted in a significant decrease in the relative density of TH-immunoreactivity and increase in the number of GFAP-positive astrocytes in the striatum of WT 129/Sv mice. The same treatment also decreased number of HuC/D-positive cells and signals of TH or ChAT, and increased signal of GFAP in the colonic myenteric plexus. Furthermore, administration of rotenone markedly increased the number of MT-positive signals in the myenteric astroglial cells of WT mice. Compared with WT mice, MT depletion exacerbated subcutaneous rotenone infusion-induced neurodegeneration in ENS, coinciding with significant decrease in colonic GFAP-immunoreactivity. Moreover,

4HNE-immunoreactivity which is considered as an index of lipid peroxidation in the myenteric plexus was notably increased by rotenone administration in MT KO mice than WT mice. Besides, previous report demonstrated that 4HNE could induce MT transcription in astrocyte (Braithwaite et al. 2010). These results imply that rotenone-induced neurodegeneration accompanying enhancement of lipid peroxidation were aggravated by the deficiency of MT. Thus, it is assumed that MT in the myenteric astroglial cells could protect neurons against rotenone-induced neuronal damages by preventing oxidative stress. A previous in vitro study showed that MT can suppress not only oxidative stress, but also apoptosis and α-synuclein expression induced by rotenone exposure (Reinecke et al. 2006). However, further studies are needed to elucidate the neuroprotective profile of MT and myenteric astroglial cells in ENS, especially against long-term systemic administration of rotenone, by more quantitative analysis using whole-mount immunostaining.

Although MT is predominately expressed and released in/from astrocytes, small amount of intrinsic MT is expressed even in neurons (Hidalgo J et al., 1994). Therefore, we examined role of MT in the rotenone-induced neurotoxicity. In the present study, primary cultured mesencephalic neurons from MT KO mice were more vulnerable to the rotenone toxicity than those from WT mice (data not shown). The rotenone-induced toxicity in neurons from MT KO mice was restored by replacement with MT. These results also suggest that MT protects neurons from rotenone-induced neurotoxicity.

In conclusion, long-term subcutaneous systemic administration of rotenone caused not only myenteric neurodegeneration with marked expression of MT in the colon but not striatal dopaminergic neuronal damage. The toxin-induced myenteric neuronal damage was exacerbated by MT deficiency, accompanied with reduction in astroglial cells activation and enhancement of oxidative stress. These findings suggest that the neuronal damage in ENS induced by systemic administration of rotenone represents region-specific vulnerability to the

toxin. The findings also suggest that the expression of MT in astroglial cells protects myenteric neurons from rotenone-induced neuronal damage. Taken together with the neuroprotective effects of MT in striatal astrocytes described in previous studies (Miyazaki et al. 2011; 2013) and our culture study, therefore, MT seems to be a suitable target for neuroprotective strategies against pathologies affecting both the CNS and ENS in PD.

Acknowledgments

This work was supported by Grants-in-Aid for Scientific Research (C) (KAKENHI #21591082, #22590934, #25461279) from Japan Society for the Promotion of Science, by Grant-in Aid for Scientific Research on Innovative Areas "Brain Environment" (KAKENHI #24111533) from the Japanese Ministry of Education, Culture, Sports, Science and Technology, and by a Research Grant from the Okayama Medical Foundation.

All authors have no actual or potential conflicts of interest, including financial, personal or other relationships with other people or organizations.

References

Asanuma M, Miyazaki I, Higashi Y, Tanaka K, Haque ME, Fujita N, Ogawa N (2002) Aggravation of 6-hydroxydopamine-induced dopaminergic lesions in metallothionein-I and -II knock-out mouse brain. Neurosci Lett 327:61-65.

Betarbet R, Sherer TB, MacKenzie G, Garcia-Osuna M, Panov AV, Greenamyre JT (2000) Chronic systemic pesticide exposure reproduces features of Parkinson's disease. Nat Neurosci 3:1301-1306.

Braak H, Del Tredici K, Rub U, de Vos RA, Jansen Steur EN, Braak E (2003) Staging of brain pathology related to sporadic Parkinson's disease. Neurobiol Aging 24:197-211.

Braithwaite EK, Mattie MD, Freedman JH (2010) Activation of metallothionein transcription by 4-hydroxynonenal. J Biochem Mol Toxicol 24:330-334.

Chung RS, Adlard PA, Dittmann J, Vickers JC, Chuah MI, West AK (2004) Neuron-glia communication: metallothionein expression is specifically up-regulated by astrocytes in response to neuronal injury. J Neurochem 88:454-461.

Dhillon AS, Tarbutton GL, Levin JL, Plotkin GM, Lowry LK, Nalbone JT, Shepherd S (2008) Pesticide/environmental exposures and Parkinson's disease in East Texas. J Agromedicine 13:37-48.

Drolet RE, Cannon JR, Montero L, Greenamyre JT (2009) Chronic rotenone exposure reproduces Parkinson's disease gastrointestinal neuropathology. Neurobiol Dis 36:96-102.

Durrenberger PF, Filiou MD, Moran LB, Michael GJ, Novoselov S, Cheetham ME, Clark P, Pearce RK, Graeber MB (2009) DnaJB6 is present in the core of Lewy bodies and is highly up-regulated in parkinsonian astrocytes. J Neurosci Res 87:238-245.

Ebadi M, Brown-Borg H, El Refaey H, Singh BB, Garrett S, Shavali S, Sharma SK (2005) Metallothionein-mediated neuroprotection in genetically engineered mouse models of

Parkinson's disease. Brain Res Mol Brain Res 134:67-75.

Fleming SM, Zhu C, Fernagut PO, Mehta A, DiCarlo CD, Seaman RL, Chesselet MF (2004) Behavioral and immunohistochemical effects of chronic intravenous and subcutaneous infusions of varying doses of rotenone. Exp Neurol 187:418-429.

Futakawa N, Kondoh M, Ueda S, Higashimoto M, Takiguchi M, Suzuki S, Sato M (2006) Involvement of oxidative stress in the synthesis of metallothionein induced by mitochondrial inhibitors. Biol Pharm Bull 29:2016-2020.

Greene JG, Noorian AR, Srinivasan S (2009) Delayed gastric emptying and enteric nervous system dysfunction in the rotenone model of Parkinson's disease. Exp Neurol 218:154-161.

Heneka MT, Rodriguez JJ, Verkhratsky A (2010) Neuroglia in neurodegeneration. Brain Res Rev 63:189-211.

Hidalgo J, García A, Oliva AM, Giralt M, Gasull T, González B, Milnerowicz H, Wood A, Bremner I (1994) Effect of zinc, copper and glucocorticoids on metallothionein levels of cultured neurons and astrocytes from rat brain. Chem Biol Interact 93:197-219.

Hubbard PS, Esiri MM, Reading M, McShane R, Nagy Z (2007) Alpha-synuclein pathology in the olfactory pathways of dementia patients. J Anat 211:117-124.

Ishida Y, Nagai A, Kobayashi S, Kim SU (2006) Upregulation of protease-activated receptor-1 in astrocytes in Parkinson disease: astrocyte-mediated neuroprotection through increased levels of glutathione peroxidase. J Neuropathol Exp Neurol 65:66-77.

Jessen KR, Mirsky R (1983) Astrocyte-like glia in the peripheral nervous system: an immunohistochemical study of enteric glia. J Neurosci 3:2206-2218.

Kondoh M, Inoue Y, Atagi S, Futakawa N, Higashimoto M, Sato M (2001) Specific induction of metallothionein synthesis by mitochondrial oxidative stress. Life Sci

69:2137-2146.

Masters BA, Kelly EJ, Quaife CJ, Brinster RL, Palmiter RD (1994) Targeted disruption of metallothionein I and II genes increases sensitivity to cadmium. Proc Natl Acad Sci USA 91: 584-588.

Michael GJ, Esmailzadeh S, Moran LB, Christian L, Pearce RK, Graeber MB (2011) Up-regulation of metallothionein gene expression in parkinsonian astrocytes. Neurogenetics 12:295-305.

Miyazaki I, Asanuma M, Hozumi H, Miyoshi K, Sogawa N (2007) Protective effects of metallothionein against dopamine quinone-induced dopaminergic neurotoxicity. FEBS Lett 581:5003-5008.

Miyazaki I, Asanuma M, Kikkawa Y, Takeshima M, Murakami S, Miyoshi K, Sogawa N, Kita T (2011) Astrocyte-derived metallothionein protects dopaminergic neurons from dopamine quinone toxicity. Glia 59:435-451.

Miyazaki I, Asanuma M, Murakami S, Takeshima M, Torigoe N, Kitamura Y, Miyoshi K (2013) Targeting 5-HT receptors in astrocytes to protect dopaminergic neurons in parkinsonian models. Neurobiol Dis 59:244-256.

Orimo S, Uchihara T, Nakamura A, Mori F, Kakita A, Wakabayashi K, Takahashi H (2008) Axonal alpha-synuclein aggregates herald centripetal degeneration of cardiac sympathetic nerve in Parkinson's disease. Brain 131:642-650.

Pan-Montojo F, Anichtchik O, Dening Y, Knels L, Pursche S, Jung R, Jackson S, Gille G, Spillantini MG, Reichmann H, Funk RH (2010) Progression of Parkinson's disease pathology is reproduced by intragastric administration of rotenone in mice. PLoS One 5:e8762.

Pan-Montojo F, Schwarz M, Winkler C, Arnhold M, O'Sullivan GA, Pal A, Said J, Marsico G, Verbavatz JM, Rodrigo-Angulo M, Gille G, Funk RH, Reichmann H (2012)

Environmental toxins trigger PD-like progression via increased alpha-synuclein release from enteric neurons in mice. Sci Rep 2:898.

Parker WD, Jr., Boyson SJ, Parks JK (1989) Abnormalities of the electron transport chain in idiopathic Parkinson's disease. Ann Neurol 26:719-723.

Pedersen MO, Jensen R, Pedersen DS, Skjolding AD, Hempel C, Maretty L, Penkowa M (2009) Metallothionein-I+II in neuroprotection. Biofactors 35:315-325.

Reinecke F, Levanets O, Olivier Y, Louw R, Semete B, Grobler A, Hidalgo J, Smeitink J, Olckers A, Van der Westhuizen FH (2006) Metallothionein isoform 2A expression is inducible and protects against ROS-mediated cell death in rotenone-treated HeLa cells. Biochem J 395:405-415.

Samantaray S, Knaryan VH, Guyton MK, Matzelle DD, Ray SK, Banik NL (2007) The parkinsonian neurotoxin rotenone activates calpain and caspase-3 leading to motoneuron degeneration in spinal cord of Lewis rats. Neuroscience 146:741-755.

Saravanan KS, Sindhu KM, Mohanakumar KP (2005) Acute intranigral infusion of rotenone in rats causes progressive biochemical lesions in the striatum similar to Parkinson's disease. Brain Res 1049:147-155.

Savidge TC, Newman P, Pothoulakis C, Ruhl A, Neunlist M, Bourreille A, Hurst R, Sofroniew MV (2007) Enteric glia regulate intestinal barrier function and inflammation via release of S-nitrosoglutathione. Gastroenterology 132:1344-1358.

Schapira AH, Cooper JM, Dexter D, Jenner P, Clark JB, Marsden CD (1989) Mitochondrial complex I deficiency in Parkinson's disease. Lancet 1:1269.

Schwarz J, Weis S, Kraft E, Tatsch K, Bandmann O, Mehraein P, Vogl T, Oertel WH (1996) Signal changes on MRI and increases in reactive microgliosis, astrogliosis, and iron in the putamen of two patients with multiple system atrophy. J Neurol Neurosurg Psychiatry 60:98-101.

Sherer TB, Betarbet R, Testa CM, Seo BB, Richardson JR, Kim JH, Miller GW, Yagi T, Matsuno-Yagi A, Greenamyre JT (2003) Mechanism of toxicity in rotenone models of Parkinson's disease. J Neurosci 23:10756-10764.

Sofic E, Lange KW, Jellinger K, Riederer P (1992) Reduced and oxidized glutathione in the substantia nigra of patients with Parkinson's disease. Neurosci Lett 142:128-130.

Spillantini MG, Schmidt ML, Lee VM, Trojanowski JQ, Jakes R, Goedert M (1997) Alpha-synuclein in Lewy bodies. Nature 388:839-840.

Stankovic RK, Chung RS, Penkowa M (2007) Metallothioneins I and II: neuroprotective significance during CNS pathology. Int J Biochem Cell Biol 39:484-489.

Tanner CM, Kamel F, Ross GW, Hoppin JA, Goldman SM, Korell M, Marras C, Bhudhikanok GS, Kasten M, Chade AR, Comyns K, Richards MB, Meng C, Priestley B, Fernandez HH, Cambi F, Umbach DM, Blair A, Sandler DP, Langston JW (2011) Rotenone, paraquat, and Parkinson's disease. Environ Health Perspect 119:866-872.

Wakida K, Shimazawa M, Hozumi I, Satoh M, Nagase H, Inuzuka T, Hara H (2007) Neuroprotective effect of erythropoietin, and role of metallothionein-1 and -2, in permanent focal cerebral ischemia. Neuroscience 148:105-114.

Wong GF, Gray CS, Hassanein RS, Koller WC (1991) Environmental risk factors in siblings with Parkinson's disease. Arch Neurol 48:287-289.

Figure legends

Fig. 1 Effects of chronic subcutaneous administration of rotenone on body weight and behavioral activity in C57BL mice. Time-course changes in body weight (a) and spontaneous locomotor activity (b) in C57BL mice treated with rotenone (50 mg/kg/day) or vehicle. Values are mean±SEM (n=4-7). *p<0.05 vs. vehicle-treated group.

Fig. 2 Effect of subcutaneous administration of rotenone on dopaminergic neurons, astrocytes and MT expression in the striatum of C57BL mice. Changes in the optical density of TH-immunoreactivity (a), and the number of GFAP-positive astrocytes (b) and MT-positive cells (c) in the mid-striatum (+0.6 to +1.0 mm from the bregma) after subcutaneous administration of rotenone (50 mg/kg/day) for 6 weeks. Partial colocalization of MT-immunopositive cells with GFAP-immunopositive astrocytes (d: green; GFAP, red; MT). Data are mean±SEM (n=4-5). *p<0.05 vs. vehicle-treated group. Scale bars = 500 μm (a); 50 μm (b-d).

Fig. 3 Effects of subcutaneous administration of rotenone on myenteric neurons, glial cells and MT expression in the colon of C57BL mice. Changes in integrated density of TH-positive neurons (a), GFAP-positive glial cells (b) and MT-positive signals (c) at 6 weeks after subcutaneous administration of rotenone (50 mg/kg/day). Data are mean±SEM (15-30 images/2 slices/animal, 4-5 animals/group). **p<0.01 vs. vehicle-treated group. Scale bars = 25 μm.

Fig. 4 Effects of long-term subcutaneous administration of rotenone on body weight and behavioral activity in MT KO and WT mice. Time-course changes in body weight (a) and

spontaneous locomotor activity (b) in MT KO mice and WT 129/Sv mice treated with rotenone (50 mg/kg/day) or vehicle. Values are mean±SEM (n=4-7). *p<0.05 vs. vehicle-treated WT mice, ##p<0.01 vs. vehicle-treated MT KO mice.

Fig. 5 Effects of subcutaneous administration of rotenone on nigrostriatal dopaminergic neurons in MT KO and WT mice. Changes in the number of TH-positive dopaminergic neurons in the substantia nigra (-2.8 to -3.0 mm from the bregma)(a), optical densities of TH-immunoreactivity (b) and optical density of DAT-immunoreactivity (c) in the mid-striatum (+0.6 to +1.0 mm from the bregma) at 4 weeks after rotenone administration (50 mg/kg/day). Data are mean±SEM (n=4-7). *p<0.05, **p<0.01 between two indicated groups. Scale bars = 100 μm (a); 500 μm (b, c).

Fig. 6 Effects of subcutaneous administration of rotenone on striatal astrocytes and MT expression in MT KO and WT mice. Changes in the number of GFAP-positive astrocytes (a: green) and MT-immunopositive cells (b: red) in the mid-striatum at 4 weeks after chronic rotenone infusion (50 mg/kg/day). Partial colocalization of MT-immunopositive cells and GFAP-immunopositive astrocytes (c: green; GFAP, red; MT). Data are mean±SEM (n=4-7). *p<0.05, **p<0.01 between two indicated groups. Scale bars = 50 μm.

Fig. 7 Effects of subcutaneous administration of rotenone on myenteric neurons in colon of MT KO and WT mice. Changes in the number of HuC/D-positive cells (a: red) and the integrated density of β-tubulin-positive neurons (b: green), TH-positive neurons (c: green), and ChAT-positive neurons (d: red) in the myenteric plexus of ascending colon at 4 weeks after administration of rotenone (50 mg/kg/day). Data are mean±SEM (10-30 images/2 slices/animal, 4-7 animals/group). *p<0.05, **p<0.01 between two indicated groups. Scale

bars = 25 μm.

Fig. 8 Effects of subcutaneous administration of rotenone on myenteric glial cells and MT expression in colon of MT KO and WT. Changes in the integrated density of GFAP-positive myenteric glial cells (a: red) and MT-immunoreactivity (b: green) in the myenteric plexus of ascending colon at 4 weeks after administration of rotenone (50 mg/kg/day). Colocalization of MT-immunopositive cells with GFAP-immunopositive astrocytes (c: red; GFAP, green; MT). Data are mean±SEM (10-30 images/2 slices/animal, 4-7 animals/group). *p<0.05 between two indicated groups. Scale bars = 25 μm.

Fig. 9 Lipid peroxidation in myenteric neurons induced by subcutaneous rotenone infusion. Representative images of 4HNE-immunoreactivity (a: red), double staining of 4HNE and β-tubulin (b: red, 4HNE; green, β-tubulin) and changes in ratio of integrated density of 4HNE to β-tubulin-immunopositive signals in the myenteric plexus of ascending colon at 4 weeks after administration of rotenone (50 mg/kg/day). Data are mean±SEM (10-30 images/2 slices/animal, 4-7 animals/group). *p<0.05, **p<0.01 between two indicated groups. Scale bars = 25 μm.

Fig. 10 Neuroprotective effects of MT against rotenone-induced neurotoxicity in primary cultured mesencephalic neurons. Cell viability of TH-positive dopaminergic neurons in mesencephalic culture from MT KO mice at 24 h after rotenone exposure (5 nM) with/without MT-1 recombinant protein (25 ng/ml). Data are mean±SEM (n=3-4). †p< 0.001 vs. control, §p< 0.001 vs. rotenone-treated group.

(a) body weight

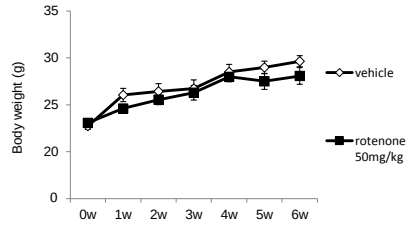

(b) spontaneous locomotor activity in open field

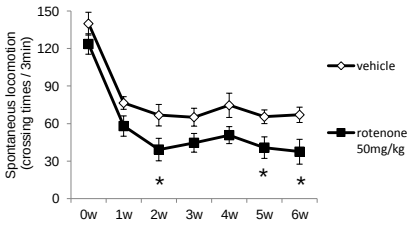

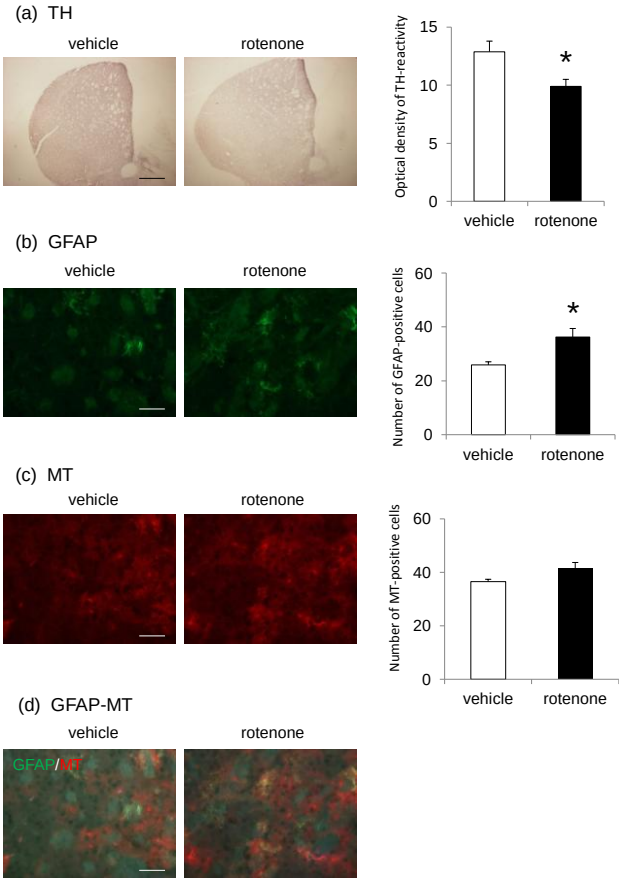
(a) TH
vehicle
rotenone
Optical density of TH-reactivity
15
10
5
0
*
vehicle
rotenone
(b) GFAP
vehicle
rotenone
Number of GFAP-positive cells
60
40
20
0
*
vehicle
rotenone
(c) MT
vehicle
rotenone
Number of MT-positive cells
60
40
20
0
vehicle
rotenone
(d) GFAP-MT
vehicle
rotenone
GFAP/MT

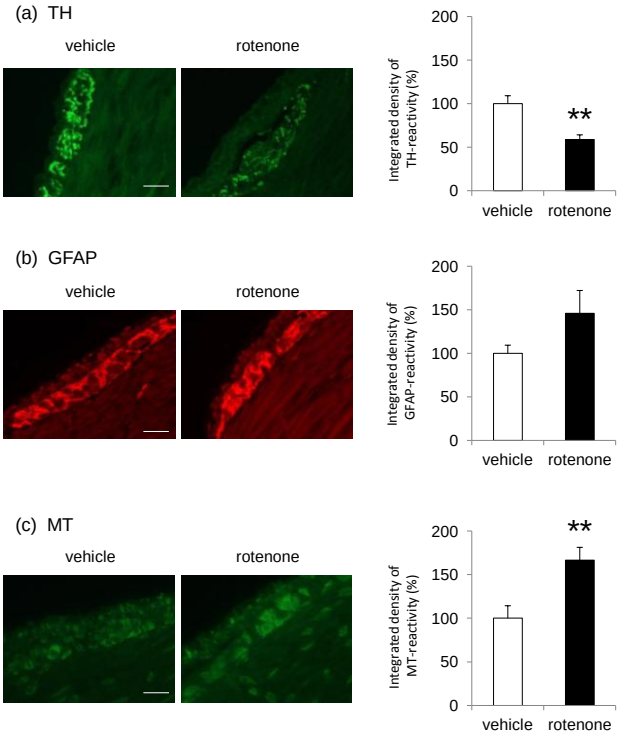
(a) TH
vehicle
rotenone
Integrated density of TH-reactivity (%)
200
150
100
50
0
**
vehicle
rotenone
(b) GFAP
vehicle
rotenone
Integrated density of GFAP-reactivity (%)
200
150
100
50
0
vehicle
rotenone
(c) MT
vehicle
rotenone
Integrated density of MT-reactivity (%)
200
150
100
50
0
**
vehicle
rotenone

(a) body weight

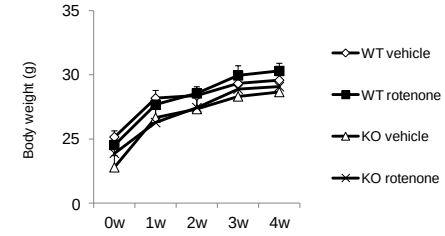

(b) spontaneous locomotor activity in open field

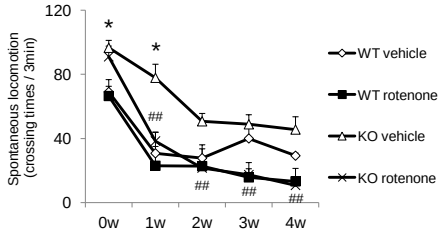

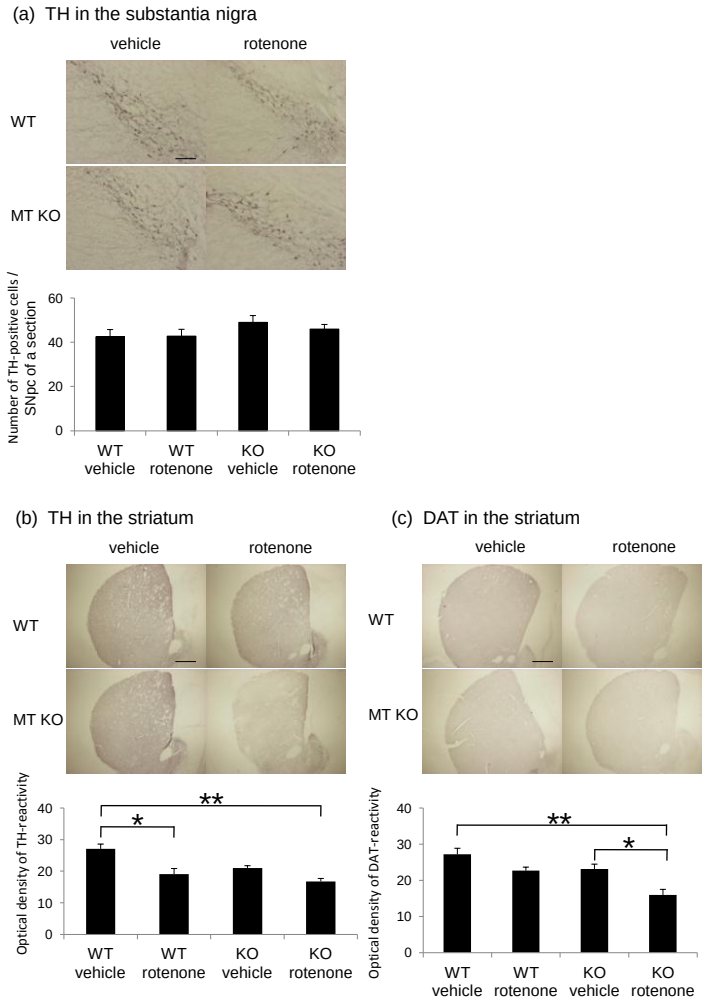
(a) TH in the substantia nigra
vehicle
rotenone
WT
MT KO
Number of TH-positive cells / SNpc of a section
60
40
20
0
WT vehicle
WT rotenone
KO vehicle
KO rotenone
(b) TH in the striatum
vehicle
rotenone
WT
MT KO
Optical density of TH-reactivity
40
30
20
10
0
*
**
WT vehicle
WT rotenone
KO vehicle
KO rotenone
(c) DAT in the striatum
vehicle
rotenone
WT
MT KO
Optical density of DAT-reactivity
40
30
20
10
0
**
*
WT vehicle
WT rotenone
KO vehicle
KO rotenone

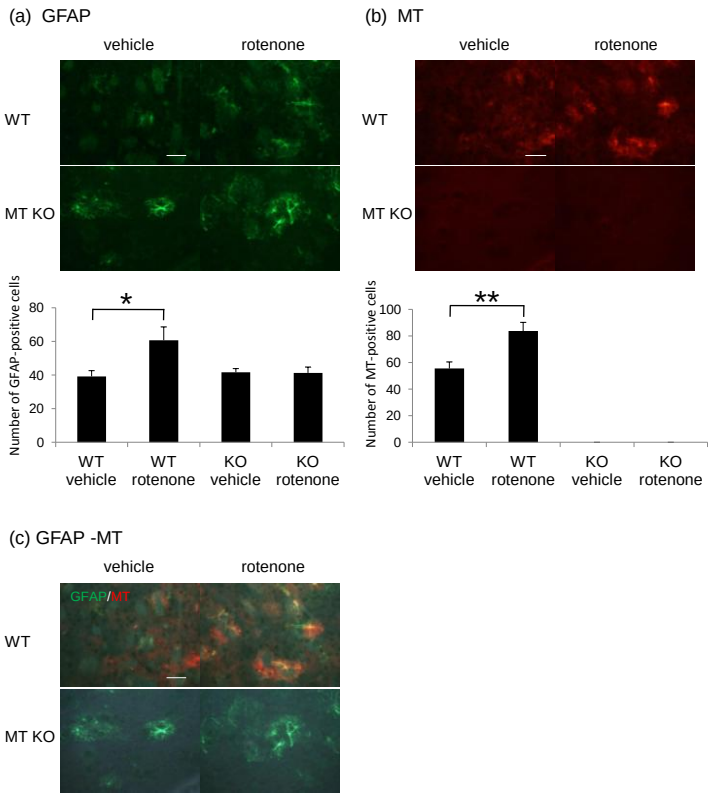
(a) GFAP
vehicle
rotenone
WT
MT KO
Number of GFAP-positive cells
80
60
40
20
0
*
WT vehicle
WT rotenone
KO vehicle
KO rotenone
(b) MT
vehicle
rotenone
WT
MT KO
Number of MT-positive cells
100
80
60
40
20
0
**
WT vehicle
WT rotenone
KO vehicle
KO rotenone

(c) GFAP -MT
vehicle
rotenone
GFAP/MT
WT
MT KO

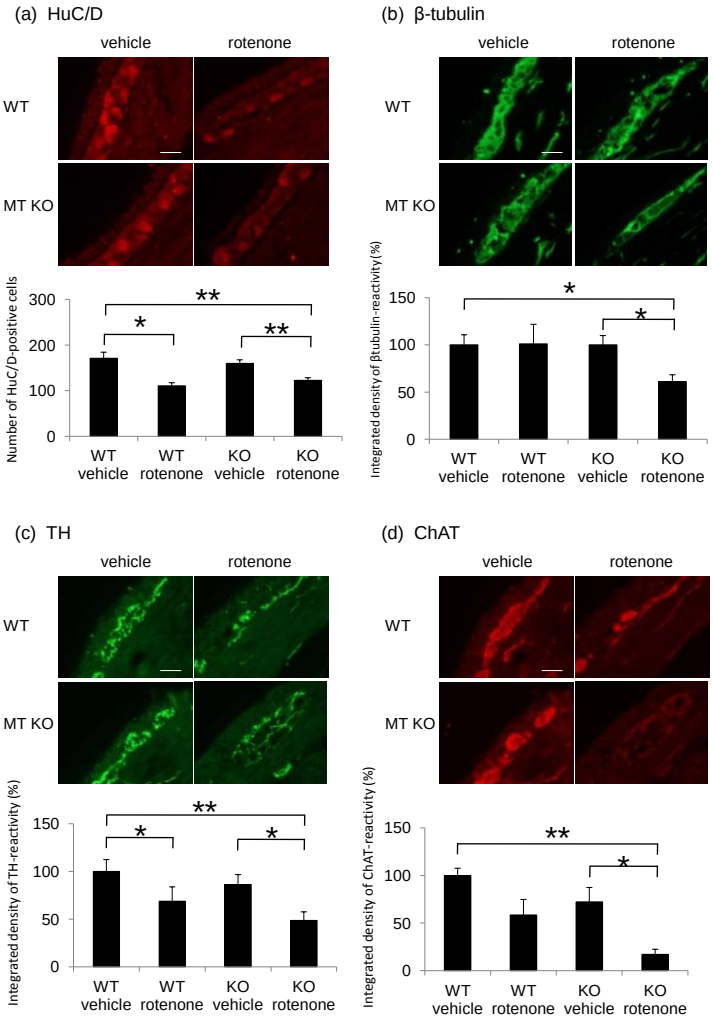
(a) HuC/D
vehicle
rotenone
WT
MT KO
Number of HuC/D-positive cells
300
200
100
0
**
*
**
WT vehicle
WT rotenone
KO vehicle
KO rotenone
(b) β-tubulin
vehicle
rotenone
WT
MT KO
Integrated density of βtubulin-reactivity (%)
150
100
50
0
*
*
WT vehicle
WT rotenone
KO vehicle
KO rotenone
(c) TH
vehicle
rotenone
WT
MT KO
Integrated density of TH-reactivity (%)
150
100
50
0
**
*
*
WT vehicle
WT rotenone
KO vehicle
KO rotenone
(d) ChAT
vehicle
rotenone
WT
MT KO
Integrated density of ChAT-reactivity (%)
150
100
50
0
**
*
WT vehicle
WT rotenone
KO vehicle
KO rotenone

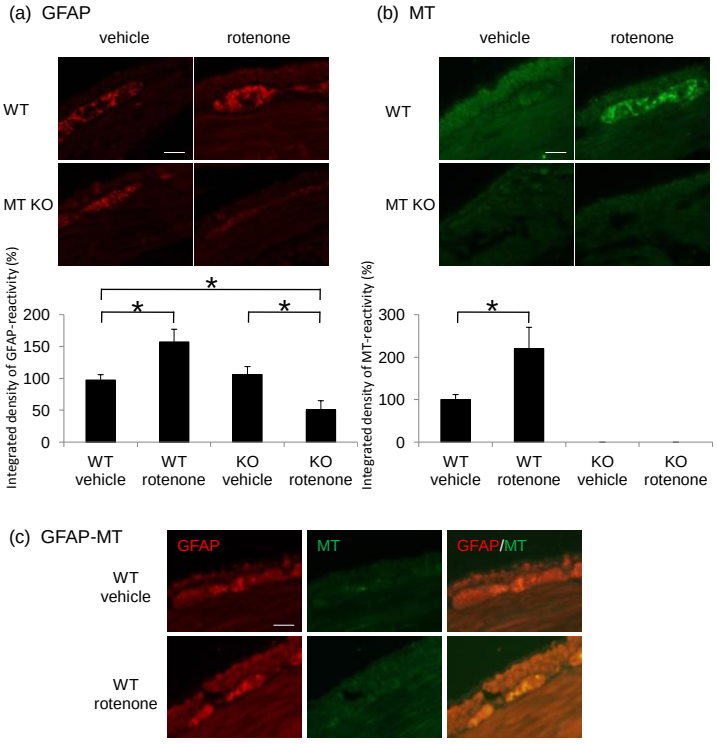
(a) GFAP
vehicle
rotenone
WT
MT KO
Integrated density of GFAP-reactivity (%)
200
150
100
50
0
*
*
*
WT vehicle
WT rotenone
KO vehicle
KO rotenone
(b) MT
vehicle
rotenone
WT
MT KO
Integrated density of MT-reactivity (%)
300
200
100
0
*
WT vehicle
WT rotenone
KO vehicle
KO rotenone

(c) GFAP-MT
GFAP
MT
GFAP/MT
WT vehicle
WT rotenone

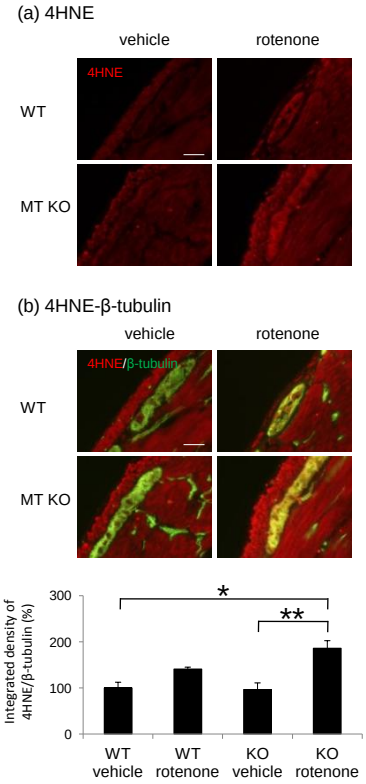
(a) 4HNE
vehicle
rotenone
4HNE
WT
MT KO
(b) 4HNE-β-tubulin
vehicle
rotenone
4HNE/β-tubulin
WT
MT KO
Integrated density of 4HNE/β-tubulin (%)
300
200
100
0
*
**
WT vehicle
WT rotenone
KO vehicle
KO rotenone

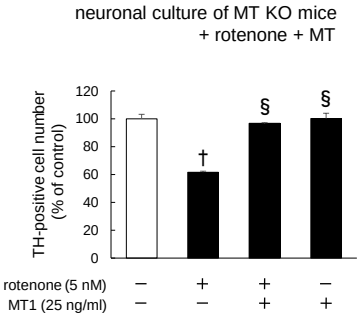
neuronal culture of MT KO mice
+ rotenone + MT
TH-positive cell number
(% of control)
120
100
80
60
40
20
0
†
§
§
rotenone (5 nM) − + + −
MT1 (25 ng/ml) − − + +